

## Article

# Preparation of Activated Carbon/TiO<sub>2</sub> Nanohybrids for Photodegradation of Reactive Red-35 Dye Using Sunlight

Bappy Mondol<sup>1</sup>, Anupam Sarker<sup>1</sup> , A. M. Shareque<sup>1</sup>, Shaikat Chandra Dey<sup>1</sup> , Mohammad Tariqul Islam<sup>2</sup> ,  
Ajoy Kumar Das<sup>1</sup>, Sayed Md. Shamsuddin<sup>1</sup> , Md. Ashraful Islam Molla<sup>1,\*</sup>  and Mithun Sarker<sup>1,\*</sup> 

- <sup>1</sup> Department of Applied Chemistry and Chemical Engineering, Faculty of Engineering and Technology, University of Dhaka, Dhaka 1000, Bangladesh; bappy279@gmail.com (B.M.); suptaaccessarker@gmail.com (A.S.); sharequetawsif@gmail.com (A.M.S.); shaikat@du.ac.bd (S.C.D.); ajoyappliedchemistry@gmail.com (A.K.D.); sdin@du.ac.bd (S.M.S.)
- <sup>2</sup> Department of Chemistry, American International University-Bangladesh, Dhaka 1229, Bangladesh; tariquidu@aiub.edu
- \* Correspondence: ashraful.acce@du.ac.bd (M.A.I.M.); mithun@du.ac.bd (M.S.); Tel.: +88-015-5235-9706 (M.A.I.M.); +88-017-9330-1288 (M.S.)

**Abstract:** Activated carbon/titanium dioxide (AC/TiO<sub>2</sub>) nanohybrids were synthesized by a hydrothermal technique using various weight percent of commercial AC and were characterized by X-ray diffraction (XRD), field emission scanning electron microscopy (FESEM), Fourier transform infrared (FTIR) and thermogravimetric analysis (TGA). The synthesized nanohybrids were applied to photodegradation of Reactive Red-35 (RR-35) dye in aqueous solution using sunlight. Due to the synergistic effect of adsorption and photodegradation activity, AC/TiO<sub>2</sub> nanohybrids were more efficient in treating the aqueous dye solution than that of AC and TiO<sub>2</sub>. The maximum (95%) RR-35 dye removal from the water was obtained with 20 wt% AC/TiO<sub>2</sub> within 30 min at natural pH of 5.6. The possible photodegradation mechanism of RR-35 dye with AC/TiO<sub>2</sub> was discussed from the scavenger test. Moreover, AC/TiO<sub>2</sub> was found to be suitable for long-term repeated applications through recyclability experiments. Therefore, AC/TiO<sub>2</sub> nanohybrid is a promising photocatalyst for treating azo dyes especially RR-35 from water.

**Keywords:** TiO<sub>2</sub>; activated carbon; nanohybrid; photodegradation; azo dyes; sunlight



**Citation:** Mondol, B.; Sarker, A.; Shareque, A.M.; Dey, S.C.; Islam, M.T.; Das, A.K.; Shamsuddin, S.M.; Molla, M.A.I.; Sarker, M. Preparation of Activated Carbon/TiO<sub>2</sub> Nanohybrids for Photodegradation of Reactive Red-35 Dye Using Sunlight. *Photochem* **2021**, *1*, 54–66. <https://doi.org/10.3390/photochem1010006>

Academic Editor: Vincenzo Vaiano

Received: 20 April 2021

Accepted: 14 May 2021

Published: 18 May 2021

**Publisher's Note:** MDPI stays neutral with regard to jurisdictional claims in published maps and institutional affiliations.



**Copyright:** © 2021 by the authors. Licensee MDPI, Basel, Switzerland. This article is an open access article distributed under the terms and conditions of the Creative Commons Attribution (CC BY) license (<https://creativecommons.org/licenses/by/4.0/>).

## 1. Introduction

Adverse effects are being observed in the environment, especially, in water quality due to the rapid urbanization and industrialization in the world. Hazardous wastes along with untreated toxic chemicals are usually flushed into rivers and ponds or nearby water reservoirs [1]. The dyes are considered hazardous water pollutants due to their toxic effects on the environment and complexity in removal [2]. Textile dyes, especially azo dyes not only affect the aesthetic merit of surface water but also reduces light penetration that hampers aquatic lives [2]. Moreover, azo dyes are usually mutagenic and carcinogenic [2,3]. Reactive Red-35 (RR-35) is a typical toxic azo dye and has widely been used in textile industries because of its vibrant colors, water-fastness and energy-efficient application techniques [4].

Several techniques have been applied for wastewater treatment, especially in azo dye removal from water [2,5]. However, the traditional physical and biological water treatment processes have some drawbacks such as prolonged tendency, high cost and lower efficiency [2]. Moreover, some non-traditional processes such as ozonation, radiation and membrane processes have some drawbacks; for example, ozonation and radiation processes generate toxic byproducts, which could be difficult to remove [6,7]. Therefore, cost-effective and environment-friendly methods are desired for the removal of toxic dyes from the effluent streams.

Photocatalytic degradation, an advanced oxidation water purification method, has attracted much interest to researchers since it can cost-effectively degrade the dyes without causing any further harm to nature [8]. To date, several metal oxides [9,10] including titanium dioxide ( $\text{TiO}_2$ ) [11] have been selected as photocatalysts due to their less toxicity, chemical stability and distinct electronic structure (unoccupied conduction band and occupied valence band) [12]. Among them,  $\text{TiO}_2$  is extensively used for a wide range of applications compared to other photocatalysts, due to its low cost, excellent aquatic stability and high redox potential [13,14]. However, some drawbacks such as easy agglomeration, lower adsorption capacity, rapid phase transformation (from highly active anatase to less active rutile phase) and separation of nano-sized  $\text{TiO}_2$  from water limit the industrial applications of  $\text{TiO}_2$  in wastewater treatment [15,16]. Therefore, the introduction of support material is needed to overcome these problems and to increase the efficiency of  $\text{TiO}_2$  [16]. Several materials including activated carbon (AC) [17], clay [18], metal-organic frameworks [19], silica [20], etc., were very commonly used as a support for  $\text{TiO}_2$ . Among them, AC is a very effective support material especially in water remediation due to its excellent hydrophobicity and high surface area with different functionalities [18]. Thus, AC would not only work as effective support material but also continuously adsorb water pollutants such as dye molecules around the surface of  $\text{TiO}_2$  to halt recombination and smooth degradation. Moreover, AC/ $\text{TiO}_2$  nanocomposites are extensively used in several purposes such as the antimicrobial agent [21], photocatalytic degradation of pharmaceutical products [22] and dye removal [17]. Therefore, the possible applications of AC/ $\text{TiO}_2$  in photocatalytic degradation of dye in water are very interesting considering the synergistic effect of the adsorption process mediated by AC and the photocatalytic activity of  $\text{TiO}_2$ .

Herein, AC/ $\text{TiO}_2$  nanohybrids were synthesized via hydrothermal technique followed by calcination. The fabricated nanohybrids were thoroughly characterized and applied as a photocatalyst for the degradation of RR-35 in aqueous solution. Moreover, the plausible mechanisms for photodegradation of RR-35 were recommended based on the radical scavenger experiments.

## 2. Materials and Methods

### 2.1. Materials

Activated carbon (AC, Darco, 100 mesh, surface area  $600 \text{ m}^2/\text{g}$ ) was purchased from Merck, Mumbai, India. Acetone (99%),  $\text{TiCl}_3$  (15%) and NaOH flakes (97%) were purchased from Loba Chemie Pvt. Ltd, Mumbai, India.  $\text{NH}_4\text{OH}$  and HCl (37%) were purchased from Merck KGaA (64271 Darmstadt, Germany).  $\text{H}_2\text{O}_2$  (35%) was collected from TCI, Tamil Nadu, India. Reactive Red-35 (RR-35) was purchased from Sisco Research Laboratories Pvt. Ltd. (SRL), Mumbai, India. All the chemicals are reagent grade and utilized without further purification.

### 2.2. Preparation of AC/ $\text{TiO}_2$ Nanohybrids

In this study, the various proportions of AC/ $\text{TiO}_2$  nanohybrids were successfully synthesized, according to the previous report with slight modification [23,24]. A 10 mL solution of  $\text{TiCl}_3$  in 15% HCl was hydrolyzed using 20 mL deionized water and then a dropwise addition of aqueous  $\text{NH}_4\text{OH}$  (20 mL) produced dark blue precipitate, which turned yellowish due to the addition of  $\text{H}_2\text{O}_2$  through constant stirring. After 30 min of vigorous stirring, the calculated amount of AC was added to the mixture. The obtained suspensions were left for 4 days for aging and then the precipitates were filtered, washed with distilled water followed by acetone and dried at  $60^\circ\text{C}$ . Finally, calcination was done at  $400^\circ\text{C}$  under air for 6 h to obtain desired AC/ $\text{TiO}_2$  nanohybrids. For comparison, bare  $\text{TiO}_2$  was also synthesized by a similar procedure without using AC.

### 2.3. Characterization of Studied Nanohybrids

An X-ray diffractometer (Ultima IV, Rigaku Corporation, Akishima, Japan) fitted with Cu  $K\alpha$  radiation ( $\lambda = 0.154 \text{ nm}$ ) was used to analyze the XRD patterns of the studied samples

at room temperature (25 °C). The morphological features of the samples were examined by an analytical field emission scanning electron microscope (FESEM) (JEOL JSM-6490LA, Tokyo, Japan) operating at an accelerating voltage of 20 kV. The interaction between TiO<sub>2</sub> and AC was observed by recording transmission spectra on a Fourier transform infrared spectrometer (FTIR, Shimadzu IR Prestidge-21, Japan) in the wavenumber range of 4000–400 cm<sup>-1</sup> with resolution 4 cm<sup>-1</sup> and S/N ratio of over 40,000:1. The thermal stability of the samples was inspected by recording thermograms on a thermogravimetric analyzer (TG-00260, SHIMADZU Corp, Japan), which operated within 25–800 °C with 10 °C min<sup>-1</sup> heating rate and 5 min hold time.

#### 2.4. RR-35 Dye Removal Experiments

The dye removal performance of commercial AC, bare TiO<sub>2</sub> and AC/TiO<sub>2</sub> nanohybrids were carried out at various operating conditions such as pH, time and dye concentration using a standard solution of RR-35 (at 536 λ<sub>max</sub> nm [25]) under solar irradiation in open-air. The remaining concentration of RR-35 after degradation at various conditions was measured by recording absorbance on a UV-1700 Spectrophotometer (Shimadzu, Japan). Batch experiments were performed under similar conditions on sunny days between 11:00 and 14:00 BST (Bangladesh standard time) for the investigation of the % removal of RR-35 using the studied photocatalysts (location coordinate: 23.7275 °N, 90.4019 °E; intensity of sunlight: 3.0 mW/cm<sup>2</sup>; time of year: June to August). The intensity of light was measured by a UV radiometer with a sensor of 320–420 nm wavelength (UVR-400, Iuchi Co., Osaka, Japan). For adjusting the pH of the solutions before degradation experiments, dilute HCl (0.1 M) and NaOH (0.1 M) aqueous solutions were used. It should be noted that the natural solution pH of RR-35 was 5.6. Moreover, a reusability experiment was carried out to evaluate the potential of AC/TiO<sub>2</sub> for industrial application.

### 3. Results and Discussion

#### 3.1. XRD Analysis

The XRD patterns of AC, TiO<sub>2</sub> and AC/TiO<sub>2</sub> nanohybrids are shown in Figure 1. As can be seen in Figure 1a, the XRD of AC shows two weak broad peaks at 25° and 44° corresponding to reflection in the (002) plane and the (100) plane, which indicates the existence of quartz phase at low concentration and two-dimensional reflections of disordered stacking of micrographites, respectively [26,27]. On the other hand, the XRD pattern of TiO<sub>2</sub> and AC/TiO<sub>2</sub> nanohybrids shows diffraction peaks at about 25.34°, 37.76°, 48.00°, 53.81° and 55.11° (2θ values), which could be indexed as (101), (004), (200), (105) and (211) planes, respectively, of an anatase TiO<sub>2</sub> [28,29]. It suggests that the anatase TiO<sub>2</sub> is predominantly formed in the nanohybrids when calcined at 400 °C [24]. The sharp peaks of the XRD pattern of synthesized nanohybrids acknowledge that there were no impurities present in the nanohybrids. Therefore, the XRD analysis strongly supports the successful fabrication of the nanohybrids. Interestingly, it was observed that the diffraction peak intensity was decreased and slight peak broadening was occurred in nanohybrids with increasing AC content (Figure 1b), similar to the previous report [22,23]. Therefore, the crystallite size of nanohybrids was decreased with increasing AC content. Based on the XRD results, the crystal size of the nanohybrids is determined using the Scherrer formula for the peak at 2θ = 25.15°. The crystal size of bare TiO<sub>2</sub>, 10 wt% AC/TiO<sub>2</sub>, 20 wt% AC/TiO<sub>2</sub> and 30 wt% AC/TiO<sub>2</sub> could be estimated as 26, 20, 16 and 15 nm, respectively. Notably, there was no characteristic peak that is observed in nanohybrids due to AC. The reason could be attributed to the fact that the main peak of AC might be shielded by the peak of anatase TiO<sub>2</sub> [30].

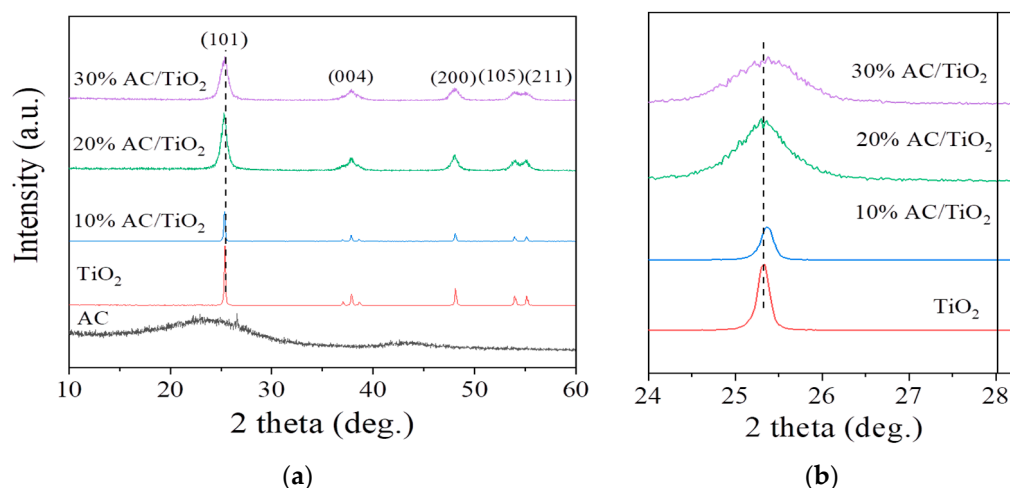


**Figure 1.** XRD pattern for (a) AC, TiO<sub>2</sub> and AC/TiO<sub>2</sub> nanohybrids and (b) elongated peak of TiO<sub>2</sub> and AC/TiO<sub>2</sub> nanohybrids.

### 3.2. FESEM Analysis

The morphologies of the AC, TiO<sub>2</sub> and AC/TiO<sub>2</sub> nanohybrids are investigated by FESEM micrographs and shown in Figure 2. The external surface of the AC clusters is flat, rough and porous whereas the aggregation of TiO<sub>2</sub> crystallites is significant in TiO<sub>2</sub>, with a size of 26 nm (based on the Scherrer equation). From FESEM images of AC/TiO<sub>2</sub> nanohybrids, it is observed that the TiO<sub>2</sub> particle with the nanosized dimension is uniformly deposited on the AC surface and in the bulk of the AC and the aggregate size of TiO<sub>2</sub> particles strongly depended on the AC content. The FESEM images, shown in Figure 2, reveal that particle size of nanohybrids decreased with increasing AC content, which is also agreeable with the XRD results. Therefore, it is easily assumed that the nanohybrid had a relatively higher percentage of smaller particles than TiO<sub>2</sub>, which might be beneficial for photocatalytic activity [31].

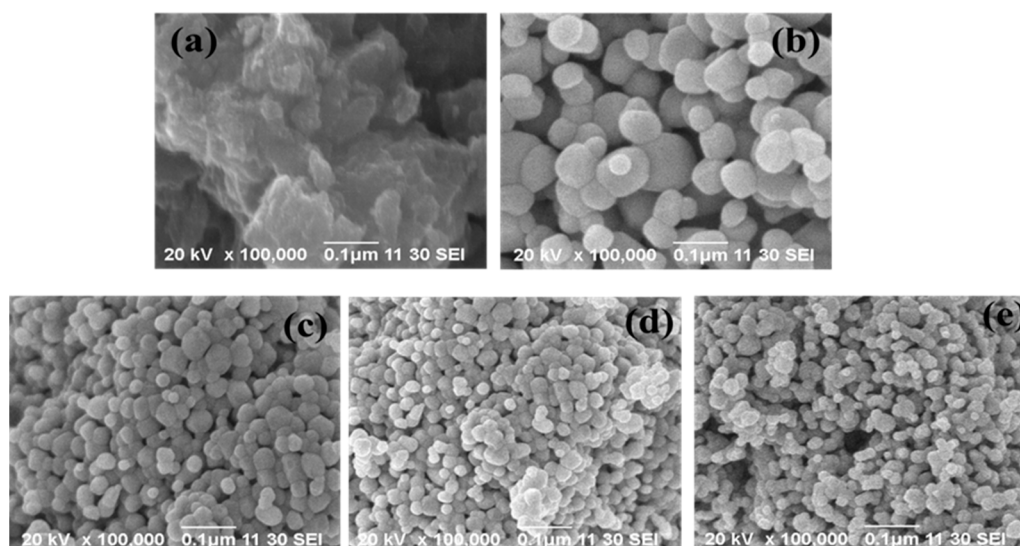


**Figure 2.** FESEM images of (a) AC, (b) TiO<sub>2</sub>, (c) 10 wt% AC/TiO<sub>2</sub>, (d) 20 wt% AC/TiO<sub>2</sub> and (e) 30 wt% AC/TiO<sub>2</sub>.

### 3.3. FTIR Analysis

FTIR spectra of TiO<sub>2</sub> and AC/TiO<sub>2</sub> nanohybrids are shown together with AC in Figure 3. The main absorption peaks were located at 3430, 1058, 710 and 530 cm<sup>-1</sup>. The

bands observed in AC and synthesized nanohybrids, located at  $3430\text{ cm}^{-1}$  were due to  $\text{-OH}$  stretching. Bare  $\text{TiO}_2$  and nanohybrids revealed an intense peak contributing to the stretching vibrations of  $\text{Ti-O}$  bonds at  $710$  and  $530\text{ cm}^{-1}$ , which is the characteristic peak of  $\text{TiO}_2$  [28]. Interestingly, with the addition of AC, a new peak located at  $1058\text{ cm}^{-1}$  appeared and the peak at  $530\text{ cm}^{-1}$  shifted to lower wavenumbers, similar to the previous report [23]. Besides, with increasing AC content, the width and intensity of the peak at  $1058\text{ cm}^{-1}$  was increased. Thus, it can be concluded that the appearance of this peak is related to AC in the AC/ $\text{TiO}_2$  composites [23].

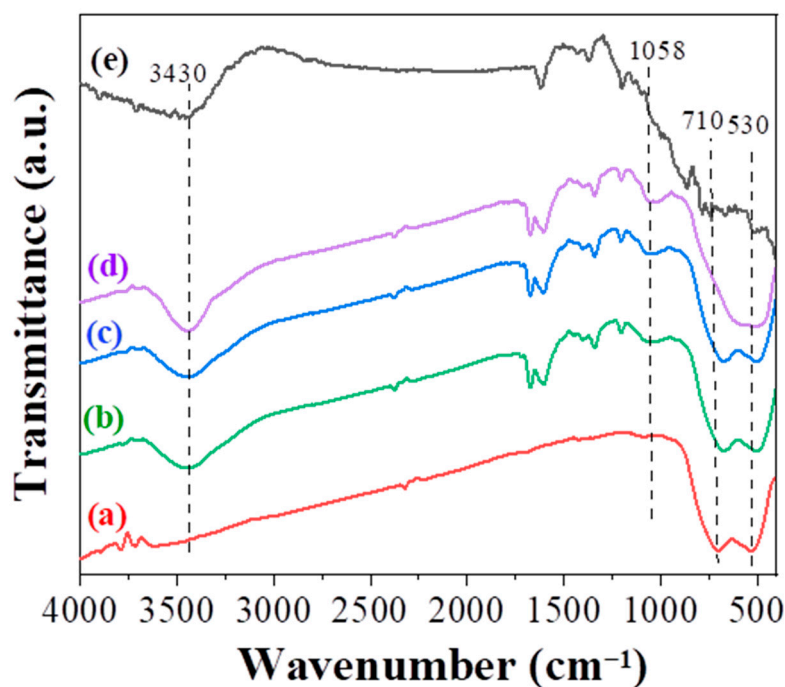


**Figure 3.** FTIR spectra of (a)  $\text{TiO}_2$ , (b) 10% AC/ $\text{TiO}_2$ , (c) 20% AC/ $\text{TiO}_2$ , (d) 30% AC/ $\text{TiO}_2$  and (e) AC.

#### 3.4. TG Analysis

To investigate the amount of  $\text{TiO}_2$  in the AC/ $\text{TiO}_2$  composites synthesized at different ratios, thermogravimetric (TG) tests were carried out in a range of  $25\text{--}800\text{ }^\circ\text{C}$  under  $\text{N}_2$  flow. As shown in the TG curves (Figure 4), the gentle weight loss of commercial AC,  $\text{TiO}_2$  and AC/ $\text{TiO}_2$  nanohybrids at temperatures ranging from  $20$  to  $200\text{ }^\circ\text{C}$  is observed due to the desorption of physisorbed water. According to the TG curves, the weight loss of the nanohybrids increased with increasing AC content. The final weight loss was  $15.6\%$  for pure AC, which is agreeable with earlier reported results [32] and  $6.6\%$ ,  $4.3\%$ ,  $2.4\%$  and  $0.60\%$  for  $30\text{ wt}\%$  AC/ $\text{TiO}_2$ ,  $20\text{ wt}\%$  AC/ $\text{TiO}_2$ ,  $10\text{ wt}\%$  AC/ $\text{TiO}_2$  and  $\text{TiO}_2$ .

#### 3.5. Effect of AC Content

The effect of AC content in nanohybrids for the removal of RR-35 from water under dark and sunlight irradiation is depicted in Figure 5. To quantify the relative contributions of both adsorption and photodegradation towards the overall removal of RR-35, control experiments in dark were carried out for  $30\text{ min}$ . As shown in Figure 5, the adsorption of RR-35 by AC,  $\text{TiO}_2$  and  $20\%$  AC/ $\text{TiO}_2$  under dark were calculated to be  $42\%$ ,  $9\%$  and  $34\%$  respectively. The respective values for commercial AC and bare  $\text{TiO}_2$  were  $47\%$  and  $26\%$  under sunlight irradiation within  $30\text{ min}$ . The removal efficiency of AC in dark and under sunlight is nearly similar which indicates that the removal of RR-35 using AC was due to adsorption rather than photocatalysis. Additionally, the  $\text{TiO}_2$  was not much effective for the degradation of RR-35 due to a large band gap, similar to the earlier report for the degradation of methyl orange dye [33]. Commercial AC showed better performance than  $\text{TiO}_2$ , which might be due to the adsorption of RR-35 on AC. Additionally, it was noticed

that the photocatalytic efficiency of nanohybrids was increased compared with commercial AC and TiO<sub>2</sub> because of the synergistic effect of both adsorption and photocatalysis due to a combination of AC and TiO<sub>2</sub> [34]. Among studied nanohybrids, 20 wt% AC/TiO<sub>2</sub> showed the best performance in RR-35 removal (95%) due to the formation of nanoparticles with good crystallinity [33]. Probably, all of the TiO<sub>2</sub> nanoparticles might take part in interaction with AC in the case of 20wt% AC/TiO<sub>2</sub>, which was important for maximum removal of RR-35 [33,35]. Therefore, further investigation was carried out using 20 wt% AC/TiO<sub>2</sub> as a photocatalyst for degradation of RR-35.

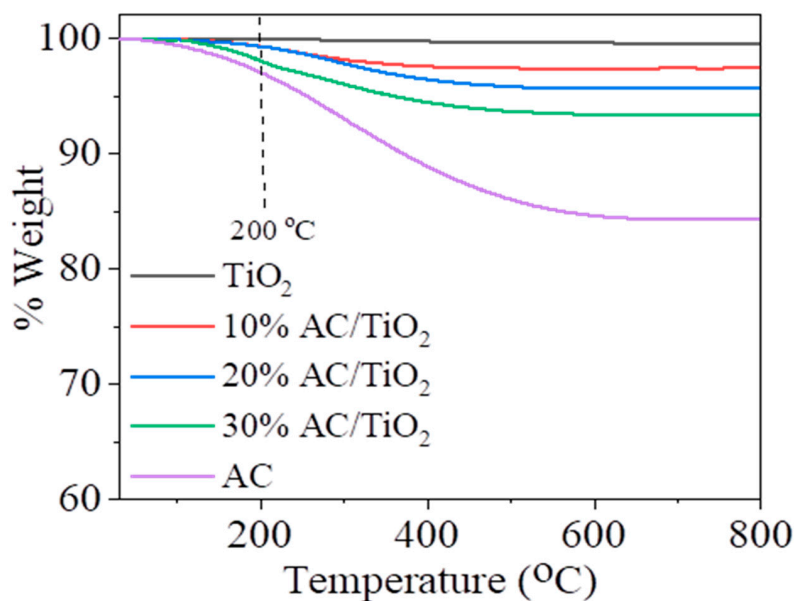


Figure 4. TGA of AC, TiO<sub>2</sub> and AC/TiO<sub>2</sub> nanohybrids.

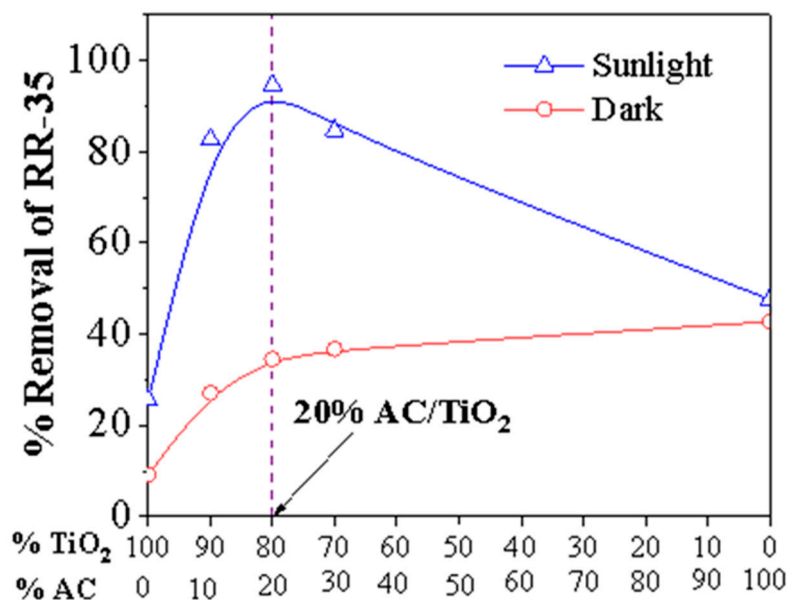
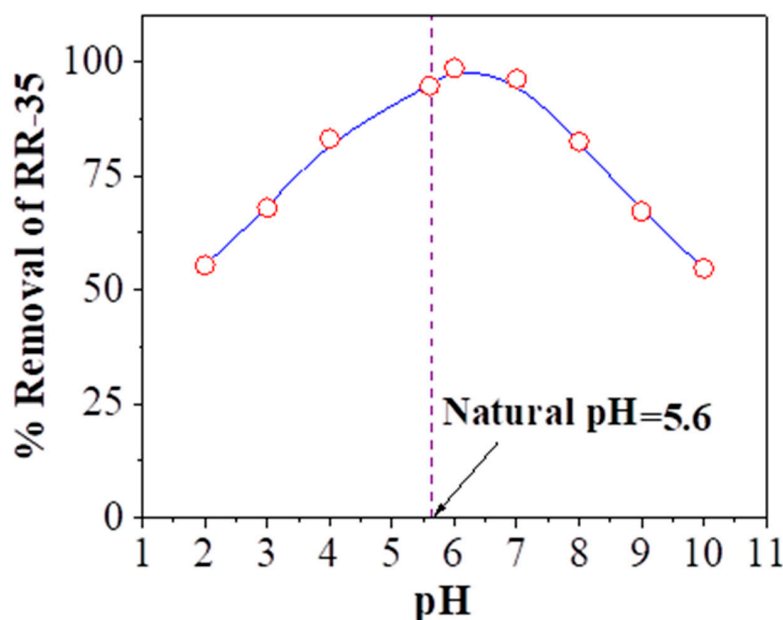


Figure 5. Effect of AC content in nanohybrids for the removal of RR-35 from water (initial concentration of RR-35: 20 mg L<sup>-1</sup>; pH: 5.6) under dark and sunlight irradiation (time: 30 min).

### 3.6. Effect of pH

Solution pH strongly controls the surface charge of a nanohybrid and thus the photodegradation of dye is also greatly affected. The degradation of RR-35 by 20 wt% AC/TiO<sub>2</sub> was recorded within a pH range of 2–10 and the results are displayed in Figure 6. The

results revealed that the degradation of dye increased with solution pH up to a certain level (at pH 6.0) and then decreased with solution pH. The maximum removal of RR-35 at pH 6.0 was 99%, after 30 min of the sunlight irradiation. At natural pH 5.6, the RR-35 removal was observed 95%, which was almost similar to the percent of removal obtained at pH 6.0. Therefore, further investigation such as the effect of time, dye concentration, scavenger test and reusability experiment was carried at natural solution pH (5.6) of RR-35. The point of zero charge value (pzc) of  $\text{TiO}_2$  and AC/ $\text{TiO}_2$  is reported as 6.8 and 7.6 respectively [25,36], which means that the surface of AC/ $\text{TiO}_2$  becomes positive below this pH value ( $\text{pH} < 7.6$ ) and negative above this pH value ( $\text{pH} > 7.6$ ). RR-35 is an anionic dye in aqueous solution; therefore, at pH 5.6–7.0, the positively charged 20 wt% AC/ $\text{TiO}_2$  surface could adsorb more dye molecules through electrostatic interaction. Due to the enhanced adsorption, more dye molecules are exposed to the active sites of the photocatalyst. The lower rate of photodegradation of RR-35 at alkaline media was found probably due to the presence of superfluous negative charge on the catalyst surface, which could repel the anionic dye molecules. Moreover, at a very low pH (from 2.0 to 4.0) the photodegradation of RR-35 decreased probably due to the protonation of dye molecules, which consequently reduced the adsorption of dye molecules on the AC/ $\text{TiO}_2$  surface [36].



**Figure 6.** Effect of pH on the removal of RR-35 with 20 wt% AC/ $\text{TiO}_2$  (initial concentration of RR-35:  $20 \text{ mg/L}^{-1}$ ; pH: 2–10; irradiation time: 30 min).

### 3.7. Effect of Time

The effect of irradiation time on photodegradation of RR-35 using 20 wt% AC/ $\text{TiO}_2$  was investigated by evaluating the percentage removal of RR-35 at different periods as shown in Figure 7. The result from Figure 7 revealed that 95% dye was removed by 5 mg of 20 wt% AC/ $\text{TiO}_2$  in 30 min at pH 5.6 under sunlight irradiation. It was evident that the rate of degradation was higher during the initial stage (up to 10 min). Afterward, the degradation rate started decreasing gradually and the degradation finally reached equilibrium after 30 min. It might be due to the gradual decline in the concentration of RR-35 and simultaneous formation of degradation products with irradiation time. As a result, maximum degradation (95%) of RR-35 was found after 30 min of sunlight irradiation.

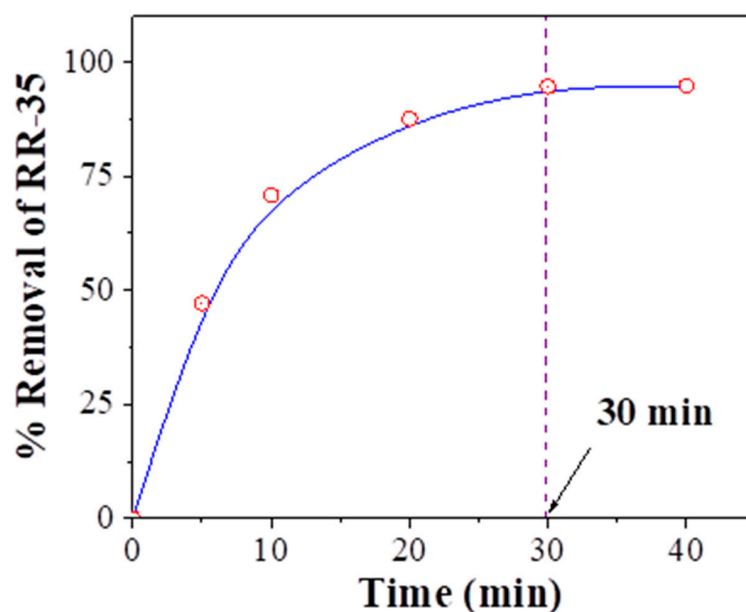


**Figure 7.** Effect of time on the removal of RR-35 with 20 wt% AC/TiO<sub>2</sub> (concentration of RR-35: 20 mg L<sup>-1</sup>; pH: 5.6; irradiation time: 0–30 min).

### 3.8. Effect of Initial Concentration of RR-35

It is necessary to study the dependence of the dye removal efficiency on the initial dye concentration given its practical application. The dye removal rate of different initial RR-35 concentrations with 20 wt% AC/TiO<sub>2</sub> is presented in Figure 8. From Figure 8 it was observed that the dye removal rate rises with the increase in initial dye concentration from 10 to 20 mg L<sup>-1</sup> and a further increase in dye concentration leads to the decrease in removal rate [37]. Additionally, with increasing the initial dye concentration up to 40 mg L<sup>-1</sup>, the degradation amounts of RR-35 increased gradually, and exceeding 40 mg L<sup>-1</sup>, the degradation amounts of RR-35 were almost the same. The high concentration gradient provides an increase of driving force to move RR-35 from the bulk to the nanohybrid surface. This mass transfer process continued until the nanohybrid surface was saturated with RR-35 molecules [38]. It could be stated that saturation probably occurred at 40 mg L<sup>-1</sup> RR-35 concentration. Besides, at a concentration above 40 mg L<sup>-1</sup>, a significant amount of sunlight may be absorbed by the dye molecules itself, which could reduce the photodegradation efficiency of AC/TiO<sub>2</sub> [39]. In this study, 20 mg L<sup>-1</sup> of RR-35 solution was selected to evaluate the photodegradation of dye for the following experiment owing to the concentration of real wastewater.

### 3.9. Role of Radical Scavenger

Radical scavenger experiments were carried out to determine the reactive species responsible for the photodegradation of RR-35 dye. In this study, iso-propanol (IP), ascorbic acid (AA) and oxalic acid (OA) were introduced to be the scavengers of hydroxyl radicals ( $\bullet\text{OH}$ ), superoxide radical ( $\bullet\text{O}_2^-$ ) and holes ( $\text{h}^+$ ), respectively [18,40–42]. The three scavenging experiments were similar to the RR-35 dye removal process. The effect of the radical scavengers on the RR-35 photodegradation over 20 wt% AC/TiO<sub>2</sub> using sunlight is displayed in Figure 9. From the figure, 95% removal of RR-35 was found with no scavenger (NS), while 56% removal was found with IP, 78% with AA and 85% with OA, respectively. The results strongly indicated that both  $\bullet\text{OH}$  and  $\bullet\text{O}_2^-$  radicals played a significant role in the photodegradation of RR-35, whereas,  $\text{h}^+$  showed a minor effect in the degradation process under sunlight.

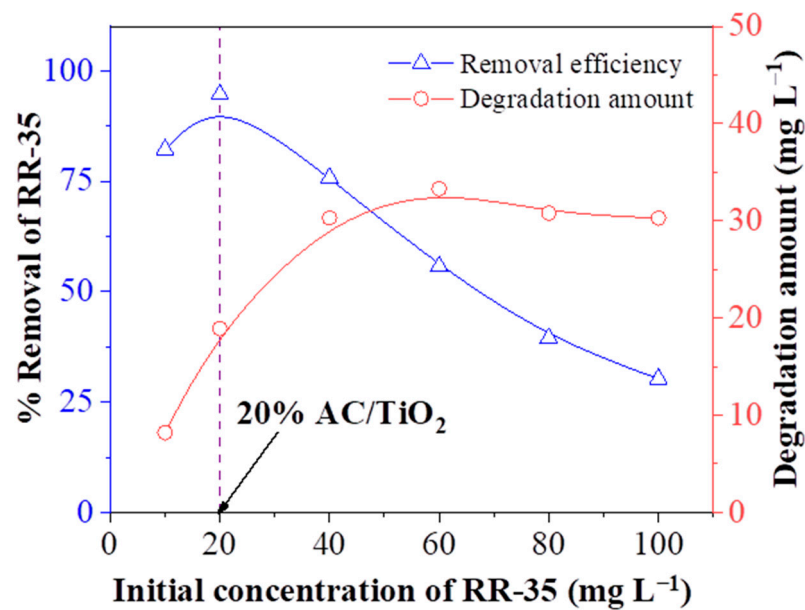


**Figure 8.** Effect of initial dye concentration on the removal of RR-35 with 20 wt% AC/TiO<sub>2</sub> (concentration of RR-35: 10–100 mg L<sup>-1</sup>; pH: 5.6; irradiation time: 30 min).

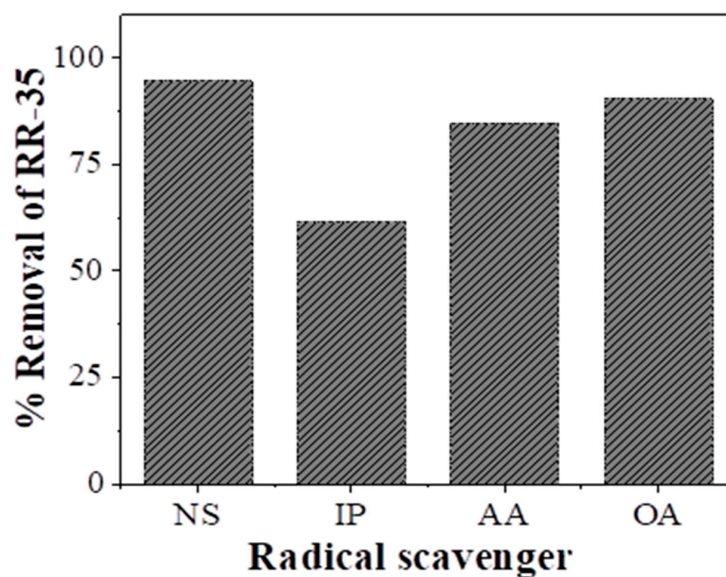


**Figure 9.** Role of radical scavengers on the RR-35 photodegradation with 20 wt% AC/TiO<sub>2</sub> (concentration of RR-35: 20 mg L<sup>-1</sup>; concentration of all scavengers: 1 mmol L<sup>-1</sup>, pH: 5.6; irradiation time: 30 min).

### 3.10. Photodegradation Mechanism

The fundamental mechanism of the AC/TiO<sub>2</sub> nanohybrids exhibit dual functions such as absorption and photodegradation to remove the RR-35 dye from an aqueous solution [34]. The proposed schematic illustration of the photodegradation mechanism of RR-35 dye by 20 wt% AC/TiO<sub>2</sub> using sunlight is presented in Figure 10. Under sunlight irradiation, the RR-35 removal process requires the dye to be adsorbed on the AC/TiO<sub>2</sub> surface before immediate photodegradation [43]. The efficiency of photodegradation can be affected by the adsorption performance of substrate AC and the photocatalytic activity of TiO<sub>2</sub> nanoparticles [34]. Moreover, the AC introduced to the composite structure acts as an electron sink, thereby decreasing the recombination of photogenerated charge carriers and finally enhancing the photocatalytic activity of the AC/TiO<sub>2</sub> [44]. During the sunlight

irradiation, the AC/TiO<sub>2</sub> (considering the semiconductor of TiO<sub>2</sub>, 3.2 eV) can absorb the UV light energy to create the conduction band electrons (e<sub>CB</sub><sup>-</sup>) and valence band holes (h<sub>VB</sub><sup>+</sup>) [30,45]. Then, the photogenerated holes (h<sub>VB</sub><sup>+</sup>) are responsible for the oxidation of RR-35 dyes and water (H<sub>2</sub>O) molecules adsorbed on the surface of the AC/TiO<sub>2</sub> and the formation of hydroxyl radicals (•OH) [44]. The photoexcited e<sub>CB</sub><sup>-</sup> attack the dissolved oxygen (O<sub>2</sub>) to generate superoxide radicals (•O<sub>2</sub><sup>-</sup>), which can act as a precursor of many reactive species in photochemical reactions [46]. Moreover, •O<sub>2</sub><sup>-</sup> is an important source of •OH radical and avoids the recombination of the electron/hole pair in the photocatalyst, thus improving the photodegradation process [47]. The photogenerated holes (h<sub>VB</sub><sup>+</sup>), photoexcited electrons (e<sub>CB</sub><sup>-</sup>), hydroxyl radicals (•OH) and superoxide radical ions (•O<sub>2</sub><sup>-</sup>) take part in heterogeneous-photocatalytic reactions. These species can lead to the photodegradation of RR-35 molecules to intermediates, and then go further degradation to CO<sub>2</sub> and H<sub>2</sub>O. Thus, the photodegradation of dye pollutants is one of the suitable processes because of its abundance advantages, such as breaking down pollutants and achieving complete mineralization to convert into non-toxic products [44]. Therefore, we expect the following photodegradation reactions of RR-35 dye by AC/TiO<sub>2</sub> under sunlight irradiation [45,47,48]:

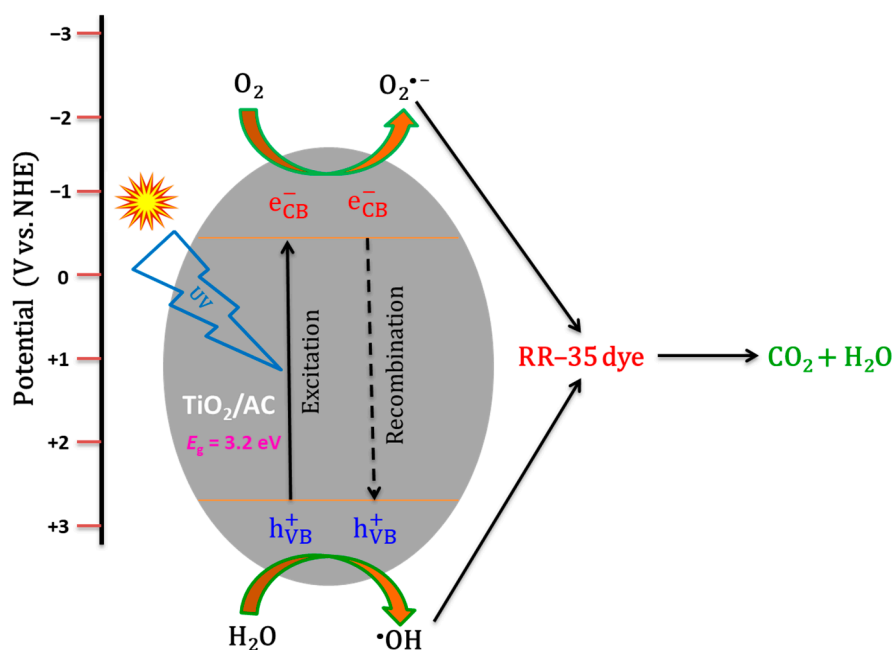
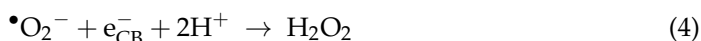
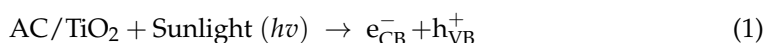


**Figure 10.** Schematic illustration of the photodegradation mechanism of RR-35 by 20 wt% AC/TiO<sub>2</sub> using sunlight.

### 3.11. Reusability of AC/TiO<sub>2</sub>

Reusability is one of the most important characteristics of a material for removing pollutants from industrial effluents since it is related to the cost-effectiveness of the photocatalyst. The reusability of 20 wt% AC/TiO<sub>2</sub> was evaluated up to four cycles by simple alkali (0.01 M NaOH) washing [34]. The alkali-treated nanohybrid was washed with distilled water and dried for the next cycle. The result of the reusability experiment is illustrated in Figure 11. The graph clearly illustrated that the performance of the recycled 20 wt%

AC/TiO<sub>2</sub> for RR-35 removal remained almost consistent. The removal activity of the nanohybrid gradually decreased up to four cycles due to the poisoning effect of degraded products and the blocking of sunlight irradiation [49]. Therefore, it can be concluded that the AC/TiO<sub>2</sub> is suitable for long-term repeated use for the removal of RR-35 dye from the aqueous environment.

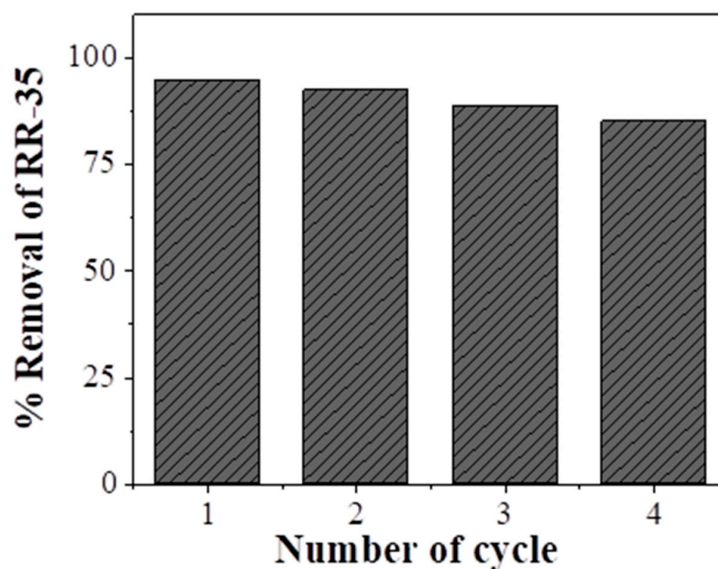


**Figure 11.** Reusability of 20 wt% AC/TiO<sub>2</sub> for RR-35 dye removal from water (concentration of RR-35: 20 mg L<sup>-1</sup>; pH: 5.6; irradiation time: 30 min).

#### 4. Conclusions

In this study, a cost-effective method has been reported for the preparation of AC/TiO<sub>2</sub> nanohybrids. The best removal efficiency for RR-35 dye was obtained by 20 wt% AC/TiO<sub>2</sub>. The remarkable removal of RR-35 with AC/TiO<sub>2</sub> can be explained by both the adsorption and photodegradation activity of nanohybrids. RR-35 dye photodegradation with AC/TiO<sub>2</sub> using sunlight was mainly controlled by the •OH and •O<sub>2</sub><sup>-</sup> radicals whereas, the h<sup>+</sup> played a minor effect in the process. Moreover, AC/TiO<sub>2</sub> nanohybrids can be regenerated by simple alkali washing. Therefore, AC/TiO<sub>2</sub> can be suggested as an efficient photocatalyst for RR-35 dye removal from water based on the facile synthesis, very fast with nearly complete removal, and excellent reusability.

**Author Contributions:** Conceptualization, M.A.I.M. and M.S.; methodology, B.M.; software, A.S. and A.M.S.; validation, B.M.; formal analysis, M.T.I., S.M.S., M.A.I.M. and M.S.; investigation, B.M.; resources, A.K.D.; data curation, B.M.; writing—original draft preparation, B.M., A.S., A.M.S. and S.C.D.; writing—review and editing, S.C.D., M.T.I., A.K.D., M.A.I.M. and M.S.; visualization, A.S., A.M.S. and S.M.S.; supervision, A.K.D.; project administration, A.K.D. All authors have read and agreed to the published version of the manuscript.

**Funding:** This research received no external funding.

**Data Availability Statement:** The data presented in this study are available in article.

**Acknowledgments:** The first author is grateful to the Ministry of Science and Technology, Bangladesh for providing the National Science and Technology Fellowship as a motivation for conducting this research. We are thankful to the Centre for Advanced Research in Sciences (CARS), Dhaka, Bangladesh for providing partial analytical support to carry out this research.

**Conflicts of Interest:** The authors declare no conflict of interest.

## References

1. Wang, Q.; Yang, Z. Industrial water pollution, water environment treatment, and health risks in China. *Environ. Pollut.* **2016**, *218*, 358–365. [[CrossRef](#)] [[PubMed](#)]
2. Katheresan, V.; Kannedo, J.; Lau, S.Y. Efficiency of various recent wastewater dye removal methods: A review. *J. Environ. Chem. Eng.* **2018**, *6*, 4676–4697. [[CrossRef](#)]
3. Alves de Lima, R.O.; Bazo, A.P.; Salvadori, D.M.F.; Rech, C.M.; de Palma Oliveira, D.; de Aragão Umbuzeiro, G. Mutagenic and carcinogenic potential of a textile azo dye processing plant effluent that impacts a drinking water source. *Mutat. Res.* **2007**, *626*, 53–60. [[CrossRef](#)] [[PubMed](#)]
4. Srinivasan, S.V.; Murthy, D.V.S. Statistical optimization for decolorization of textile dyes using *Trametes versicolor*. *J. Hazard. Mater.* **2009**, *165*, 909–914. [[CrossRef](#)]
5. Mezohegyi, G.; van der Zee, F.P.; Font, J.A.; Fortuny, A.; Fabregat, A. Towards advanced aqueous dye removal processes: A short review on the versatile role of activated carbon. *J. Environ. Manag.* **2012**, *102*, 148–164. [[CrossRef](#)] [[PubMed](#)]
6. Ike, I.A.; Lee, Y.; Hur, J. Impacts of advanced oxidation processes on disinfection byproducts from dissolved organic matter upon post-chlor(am)ination: A critical review. *Chem. Eng. J.* **2019**, *375*, 121929. [[CrossRef](#)]
7. Sarker, M.; Bhadra, B.N.; Seo, P.W.; Jhung, S.H. Adsorption of benzotriazole and benzimidazole from water over a Co-based metal azolate framework MAF-5(Co). *J. Hazard. Mater.* **2017**, *324*, 131–138. [[CrossRef](#)] [[PubMed](#)]
8. Zangeneh, H.; Zinatizadeh, A.A.L.; Habibi, M.; Akia, M.; Isa, M.H. Photocatalytic oxidation of organic dyes and pollutants in wastewater using different modified titanium dioxides: A comparative review. *J. Ind. Eng. Chem.* **2015**, *26*, 1–36. [[CrossRef](#)]
9. Gusain, R.; Gupta, K.; Joshi, P.; Khatir, O.P. Adsorptive removal and photocatalytic degradation of organic pollutants using metal oxides and their composites: A comprehensive review. *Adv. Colloid Interface Sci.* **2019**, *272*, 102009. [[CrossRef](#)]
10. Gnanasekaran, L.; Hemamalini, R.; Saravanan, R.; Ravichandran, K.; Gracia, F.; Agarwal, S.; Gupta, V.K. Synthesis and characterization of metal oxides (CeO<sub>2</sub>, CuO, NiO, Mn<sub>3</sub>O<sub>4</sub>, SnO<sub>2</sub> and ZnO) nanoparticles as photo catalysts for degradation of textile dyes. *J. Photochem. Photobiol. B* **2017**, *173*, 43–49. [[CrossRef](#)]
11. Al-Amin, M.; Dey, S.C.; Rashid, T.U.; Ashaduzzaman, M.; Shamsuddin, S.M. Solar assisted photocatalytic degradation of reactive azo dyes in presence of anatase titanium dioxide. *Int. J. Latest Res. Eng. Technol.* **2016**, *2*, 14–21.
12. Dong, S.; Feng, J.; Fan, M.; Pi, Y.; Hu, L.; Han, X.; Liu, M.; Sun, J.; Sun, J. Recent developments in heterogeneous photocatalytic water treatment using visible light-responsive photocatalysts: A review. *RSC Adv.* **2015**, *5*, 14610–14630. [[CrossRef](#)]
13. Lee, S.-Y.; Park, S.-J. TiO<sub>2</sub> photocatalyst for water treatment applications. *J. Ind. Eng. Chem.* **2013**, *19*, 1761–1769. [[CrossRef](#)]
14. Paul, S.C.; Dey, S.C.; Molla, M.A.I.; Islam, M.S.; Debnath, S.; Miah, M.Y.; Ashaduzzaman, M.; Sarker, M. Nanomaterials as electrocatalyst for hydrogen and oxygen evolution reaction: Exploitation of challenges and current progressions. *Polyhedron* **2021**, *193*, 114871. [[CrossRef](#)]
15. Dong, H.; Zeng, G.; Tang, L.; Fan, C.; Zhang, C.; He, X.; He, Y. An overview on limitations of TiO<sub>2</sub>-based particles for photocatalytic degradation of organic pollutants and the corresponding countermeasures. *Water Res.* **2015**, *79*, 128–146. [[CrossRef](#)] [[PubMed](#)]
16. Chen, J.; Qiu, F.; Xu, W.; Cao, S.; Zhu, H. Recent progress in enhancing photocatalytic efficiency of TiO<sub>2</sub>-based materials. *Appl. Catal. A Gen.* **2015**, *495*, 131–140. [[CrossRef](#)]
17. Asiltürk, M.; Şener, Ş. TiO<sub>2</sub>-activated carbon photocatalysts: Preparation, characterization and photocatalytic activities. *Chem. Eng. J.* **2012**, *180*, 354–363. [[CrossRef](#)]
18. Hasan, A.K.M.M.; Dey, S.C.; Rahman, M.M.; Zakaria, A.M.; Sarker, M.; Ashaduzzaman, M.; Shamsuddin, S.M. A kaolinite/TiO<sub>2</sub>/ZnO-based novel ternary composite for photocatalytic degradation of anionic azo dyes. *Bull. Mater. Sci.* **2020**, *43*, 1–9. [[CrossRef](#)]
19. Wang, C.-C.; Wang, X.; Liu, W. The synthesis strategies and photocatalytic performances of TiO<sub>2</sub>/MOFs composites: A state-of-the-art review. *Chem. Eng. J.* **2020**, *391*, 123601. [[CrossRef](#)]
20. Sun, Z.; Bai, C.; Zheng, S.; Yang, X.; Frost, R.L. A comparative study of different porous amorphous silica minerals supported TiO<sub>2</sub> catalysts. *Appl. Catal. A Gen.* **2013**, *458*, 103–110. [[CrossRef](#)]
21. Suba, V.; Saravanabhavan, M.; Krishna, L.S.; Kaleemulla, S.; Kumar, E.R.; Rathika, G. Evaluation of curcumin assistance in the antimicrobial and photocatalytic activity of a carbon based TiO<sub>2</sub> nanocomposite. *New J. Chem.* **2020**, *44*, 15895–15907. [[CrossRef](#)]
22. Martins, A.C.; Cazetta, A.L.; Pezoti, O.; Souza, J.R.B.; Zhang, T.; Pilau, E.J.; Asefa, T.; Almeida, V.C. Sol-gel synthesis of new TiO<sub>2</sub>/activated carbon photocatalyst and its application for degradation of tetracycline. *Ceram. Int.* **2017**, *43*, 4411–4418. [[CrossRef](#)]
23. Liu, S.X.; Chen, X.Y.; Chen, X. A TiO<sub>2</sub>/AC composite photocatalyst with high activity and easy separation prepared by a hydrothermal method. *J. Hazard. Mater.* **2007**, *143*, 257–263. [[CrossRef](#)] [[PubMed](#)]
24. Ambrus, Z.; Bala'zs, N.; Alapi, T.; Wittmann, G.; Sipos, P.; Dombi, A.; Mogyorósi, K. Synthesis, structure and photocatalytic properties of Fe(III)-doped TiO<sub>2</sub> prepared from TiCl<sub>3</sub>. *Appl. Catal. B Environ.* **2008**, *81*, 27–37. [[CrossRef](#)]
25. Bansal, P.; Sud, D. Photocatalytic degradation of commercial dye, CI Reactive Red 35 in aqueous suspension: Degradation pathway and identification of intermediates by LC/MS. *J. Mol. Catal. A Chem.* **2013**, *374–375*, 66–72. [[CrossRef](#)]
26. Sarker, M.; Ahmed, I.; Jhung, S.H. Adsorptive removal of herbicides from water over nitrogen-doped carbon obtained from ionic liquid@ZIF-8. *Chem. Eng. J.* **2017**, *323*, 203–211. [[CrossRef](#)]
27. Zhu, Z.; Li, A.; Zhong, S.; Liu, F.; Zhang, Q. Preparation and characterization of polymer-based spherical activated carbons with tailored pore structure. *J. Appl. Polym. Sci.* **2008**, *109*, 1692–1698. [[CrossRef](#)]

28. Liu, Y.; Yang, S.; Hong, J.; Sun, C. Low-temperature preparation and microwave photocatalytic activity study of TiO<sub>2</sub>-mounted activated carbon. *J. Hazard. Mater.* **2007**, *142*, 208–215. [[CrossRef](#)]
29. Huang, D.; Miyamoto, Y.; Matsumoto, T.; Tojo, T.; Fan, T.; Ding, J.; Guo, Q.; Zhang, D. Preparation and characterization of high-surface-area TiO<sub>2</sub>/activated carbon by low-temperature impregnation. *Sep. Purif. Technol.* **2011**, *78*, 9–15. [[CrossRef](#)]
30. Xing, B.; Shi, C.; Zhang, C.; Yi, G.; Chen, L.; Guo, H.; Huang, G.; Cao, J. Preparation of TiO<sub>2</sub>/activated carbon composites for photocatalytic degradation of RhB under UV light irradiation. *J. Nanomater.* **2016**, *2016*, 8393648. [[CrossRef](#)]
31. Xu, Y.-J.; Zhuang, Y.; Fu, X.Z. New insight for enhanced photocatalytic activity of TiO<sub>2</sub> by doping carbon nanotubes: A case study on degradation of benzene and methyl orange. *J. Phys. Chem. C* **2010**, *114*, 2669–2676. [[CrossRef](#)]
32. Anyika, C.; Asri, N.A.M.; Majid, Z.A.; Yahya, A.; Jaafar, J. Synthesis and characterization of magnetic activated carbon developed from palm kernel shells. *Nanotechnol. Environ. Eng.* **2017**, *2*, 1–25. [[CrossRef](#)]
33. Saravanan, R.; Aviles, J.; Gracia, F.; Mosquera, E.; Gupta, V.K. Crystallinity and lowering band gap induced visible light photocatalytic activity of TiO<sub>2</sub>/CS (Chitosan) nanocomposites. *Int. J. Biol. Macromol.* **2018**, *109*, 1239–1245. [[CrossRef](#)]
34. Xue, G.; Liu, H.H.; Chen, Q.Y.; Hills, C.; Tyrer, M.; Innocent, F. Synergy between surface adsorption and photocatalysis during degradation of humic acid on TiO<sub>2</sub>/activated carbon composites. *J. Hazard. Mater.* **2011**, *186*, 765–772. [[CrossRef](#)] [[PubMed](#)]
35. Dey, S.C.; Moztahida, M.; Sarker, M.; Ashaduzzaman, M.; Shamsuddin, S.M. pH-triggered interfacial interaction of kaolinite/chitosan nanocomposites with anionic azo dye. *J. Compos. Sci.* **2019**, *3*, 39. [[CrossRef](#)]
36. Atout, H.; Bouguettoucha, A.; Chebli, D.; Gatica, J.M.; Vidal, H.; Yeste, M.P.; Amrane, A. Integration of adsorption and photocatalytic degradation of methylene blue using TiO<sub>2</sub> supported on granular activated carbon. *Arab. J. Sci. Eng.* **2017**, *42*, 1475–1486. [[CrossRef](#)]
37. Sakib, A.A.M.; Masum, S.M.; Hoinkis, J.; Islam, R.; Molla, M.A.I. Synthesis of CuO/ZnO nanocomposites and their application in photodegradation of toxic textile dye. *J. Compos. Sci.* **2019**, *3*, 91. [[CrossRef](#)]
38. Lang, X.; Wang, T.; Sun, M.; Chen, X.; Liu, Y. Advances and applications of chitosan-based nanomaterials as oral delivery carriers: A review. *Int. J. Biol. Macromol.* **2020**, *154*, 433–445. [[CrossRef](#)]
39. Molla, M.A.I.; Ahsan, S.; Tateishi, I.; Furukawa, M.; Katsumata, H.; Suzuki, T.; Kaneco, S. Degradation, kinetics, and mineralization in the solar photocatalytic treatment of aqueous amitrole solution with titanium dioxide. *Environ. Eng. Sci.* **2018**, *35*, 401–407. [[CrossRef](#)]
40. Santhosh, C.; Malathi, A.; Daneshvar, E.; Kollu, P.; Bhatnagar, A. Photocatalytic degradation of toxic aquatic pollutants by novel magnetic 3D-TiO<sub>2</sub>@HPGA nanocomposite. *Sci. Rep.* **2018**, *8*, 1–15. [[CrossRef](#)]
41. Molla, M.A.I.; Furukawa, M.; Tateishi, I.; Katsumata, H.; Kaneco, S. Fabrication of Ag-doped ZnO by mechanochemical combustion method and their application into photocatalytic Famotidine degradation. *J. Environ. Sci. Health. Part A* **2019**, *54*, 914–923. [[CrossRef](#)] [[PubMed](#)]
42. Su, J.; Zhu, L.; Geng, P.; Chen, G. Self-assembly graphitic carbon nitride quantum dots anchored on TiO<sub>2</sub> nanotube arrays: An efficient heterojunction for pollutants degradation under solar light. *J. Hazard. Mater.* **2016**, *316*, 159–168. [[CrossRef](#)] [[PubMed](#)]
43. Omri, A.; Benzina, M. Almond shell activated carbon: Adsorbent and catalytic support in the phenol degradation. *Environ. Monit. Assess.* **2014**, *186*, 3875–3890. [[CrossRef](#)] [[PubMed](#)]
44. Baca, M.; Wenelska, K.; Mijowska, E.; Kaleńczuk, R.J.; Zielińska, B. Physicochemical and photocatalytic characterization of mesoporous carbon/titanium dioxide spheres. *Diam. Relat. Mater.* **2020**, *101*, 107551. [[CrossRef](#)]
45. Molla, M.A.I.; Tateishi, I.; Furukawa, M.; Katsumata, H.; Suzuki, T.; Kaneco, S. Evaluation of reaction mechanism for photocatalytic degradation of dye with self-sensitized TiO<sub>2</sub> under visible light irradiation. *Open J. Inorg. Non-Met. Mater.* **2017**, *7*, 1–7.
46. Ahmed, A.Z.; Islam, M.M.; Islam, M.M.; Masum, S.M.; Islam, R.; Molla, M.A.I. Fabrication and characterization of B/Sn-doped ZnO nanoparticles via mechanochemical method for photocatalytic degradation of rhodamine B. *Inorg. Nano-Met. Chem.* **2020**. [[CrossRef](#)]
47. Asencios, Y.J.O.; Lourenc,o, V.S.; Carvalho, W.A. Removal of phenol in seawater by heterogeneous photocatalysis using activated carbon materials modified with TiO<sub>2</sub>. *Catal. Today* **2020**. [[CrossRef](#)]
48. Yao, S.; Li, J.; Shi, Z. Immobilization of TiO<sub>2</sub> nanoparticles on activated carbon fiber and its photodegradation performance for organic pollutants. *Particuology* **2010**, *8*, 272–278. [[CrossRef](#)]
49. Argyle, M.D.; Bartholomew, C.H. Heterogeneous catalyst deactivation and regeneration: A review. *Catalysts* **2015**, *5*, 145–269. [[CrossRef](#)]